

Physical parameters of the Small Magellanic Cloud RR Lyrae stars and the distance scale

Sukanta Deb^{1*}, Harinder P. Singh^{1,2}

¹*Department of Physics & Astrophysics, University of Delhi, Delhi 110007, India*

²*CRAL-Observatoire de Lyon, CNRS UMR 142, 69561 Saint-Genis Laval, France*

Received on ; Accepted on

ABSTRACT

We present a careful and detailed light curve analysis of RR Lyrae stars in the Small Magellanic Cloud (SMC) discovered by the Optical Gravitational Lensing Experiment (OGLE) project. Out of 536 single mode RR Lyrae stars selected from the database, we have investigated the physical properties of 335 ‘normal looking’ RRab stars and 17 RRc stars that have good quality photometric light curves. We have also been able to estimate the distance modulus of the cloud which is in good agreement with those determined from other independent methods. The Fourier decomposition method has been used to study the basic properties of these variables. Accurate Fourier decomposition parameters of 536 RR Lyrae stars in the OGLE-II database are computed. Empirical relations between the Fourier parameters and some physical parameters of these variables have been used to estimate the physical parameters for the stars from the Fourier analysis. Further, the Fourier decomposition of the light curves of the SMC RR Lyrae stars yields their mean physical parameters as: $[\text{Fe}/\text{H}] = -1.56 \pm 0.25$, $M = 0.55 \pm 0.01 M_{\odot}$, $T_{\text{eff}} = 6404 \pm 12 \text{ K}$, $\log L = 1.60 \pm 0.01 L_{\odot}$ and $M_V = 0.78 \pm 0.02$ for 335 RRab variables and $[\text{Fe}/\text{H}] = -1.90 \pm 0.13$, $M = 0.82 \pm 0.18 M_{\odot}$, $T_{\text{eff}} = 7177 \pm 16 \text{ K}$, $\log L = 1.62 \pm 0.02 L_{\odot}$ and $M_V = 0.76 \pm 0.05$ for 17 RRc stars. Using the absolute magnitude together with the mean magnitude, intensity-weighted mean magnitude and the phase-weighted mean magnitude of the RR Lyrae stars, the mean distance modulus to the SMC is estimated to be $18.86 \pm 0.01 \text{ mag}$, $18.83 \pm 0.01 \text{ mag}$ and $18.84 \pm 0.01 \text{ mag}$ respectively from the RRab stars. From the RRc stars, the corresponding distance modulus values are found to be $18.92 \pm 0.04 \text{ mag}$, $18.89 \pm 0.04 \text{ mag}$ and $18.89 \pm 0.04 \text{ mag}$ respectively. Since Fourier analysis is a very powerful tool for the study of the physical properties of the RR Lyrae stars, we emphasize the importance of exploring the reliability of the calculation of Fourier parameters together with the uncertainty estimates keeping in view the large collections of photometric light curves that will become available from variable star projects of the future.

Key words: stars: RR Lyrae : Methods : data analysis

1 INTRODUCTION

RR Lyrae (RRL) stars have played an important role in determining the cosmic distance scale in modern astronomy. While several studies have used classical Cepheids as primary distance indicators, RRL stars have received substantial attention in solving the distance scale problem. Apart from distance determinations, RRL stars are of particular importance as a test bed for the theories of stellar and galactic structure and evolution. They are the tracers of old stellar populations of the bulge, disk and halo components that are

present everywhere. RRL stars are radially pulsating A-F variable stars with periods in the 0.2 - 1.2 day range, and amplitude of variation $\leq 2 \text{ mag}$. They can be easily identified, and play a key role as the cornerstone of the Population II distance scale. They are extensively used to determine distances to old and sufficiently metal-poor systems, where they are commonly found in large numbers. In particular, RRL stars are present in globular clusters (GCs) and the dwarf galaxies in the neighborhood of the Milky Way (Greco et al. 2007), and have also been identified in the M31 field (Brown et al. 2004, Dolphin et al. 2004), in some M31 companions (Pritzl et al. 2005), and in at least four M31 GCs (Clementini et al. 2001). Distances to the Large Magellanic Cloud

* E-mail: sdeb@physics.du.ac.in

(LMC) for the population II objects are based on the luminosity of the RRL stars (Clementini et al. 2002).

There have been a very few studies to estimate the distance scale of the SMC using the RRL stars. Using four RRL light curves of the SMC cluster NGC 121, Walker & Mack (1988) have estimated the distance modulus of the cluster to be 18.86 ± 0.07 mag. On the other hand, using 22 RR Lyrae stars surveyed around 1.3 square degrees near the northeast arm of the SMC field NGC 361, Smith et al. (1992) obtained the distance modulus of the SMC as 18.90 ± 0.16 mag. Also, there are other studies of estimating the distance scale of the SMC based on the binary star light curves and double mode Cepheids. Harries et al. (2003) reported that the distance modulus to the SMC is of the order of 18.89 ± 0.14 mag taking 10 eclipsing binaries in the SMC. By selecting 40 eclipsing binaries of spectral type O and B in the SMC, Hilditch et al. (2005) have derived the fundamental parameters of the binaries and refined the distance modulus to the SMC to 18.91 ± 0.1 mag. Also Kovács et al. (2000) found the distance modulus of the SMC to be 19.05 ± 0.017 mag based on the photometric data of double-mode Cepheids from the OGLE project.

The stellar atmospheric parameters of effective temperature (T_{eff}) and surface gravity ($\log g$) are of fundamental astrophysical importance. They are the prerequisites to any detailed abundance analysis and define the physical conditions in the stellar atmosphere and hence are directly related to the physical properties mass (M), radius (R) and luminosity (L) of the star. In this paper, we present an independent analysis of 536 SMC RRL stars discovered by the OGLE project (Soszyński et al. 2002). The OGLE database is a very wealthy resource for studying the characteristics of variable stars in the Galaxy, LMC and SMC. For the first time, we make use of the OGLE SMC data to estimate the distance scale of the SMC using a large number of well-sampled RRL light curves. The road map of the present investigation is to perform a Fourier analysis of the RRL stars in order to estimate their physical parameters and hence the SMC distance scale.

We employ the Fourier decomposition technique which is used extensively to characterize the observed photometric light curves of RRL and other types of variables. The accurate determination of the Fourier coefficients is, therefore, an important task. We have performed an independent automated Fourier analysis of all the RRL light curves selected in this paper by a computer code developed by us. In section 2 we give a brief description of the database that we use and the procedure of removing the outliers from the light curve data. We present Fourier decomposition of the light curves in section 3. We also describe the use of the unit-lag auto-correlation function for finding out the optimal order of the fit to the RRL light curves. Section 4 describes the error analysis of the Fourier decomposition parameters ϕ_{11} and R_{41} . Section 5 describes the calibration of the I band data to the V band. In section 6, we describe the various physical parameters of the RRLs obtained by using empirical relations from the literature. Section 7 describes the distance determination of the SMC. Lastly, in section 8, we present the conclusions of our study.

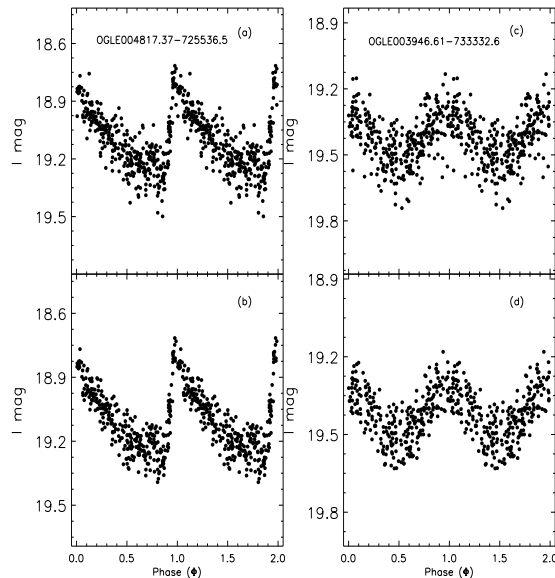


Figure 1. Examples of light curve data from the OGLE-II database (a) raw RRL light curve, (c) raw RRc light curve. In panels (b) and (d) the corresponding outlier removed smoothed light curves are shown.

2 THE OBSERVATIONAL DATABASE

The RRL stars analyzed in the present work were selected from the high quality photometric catalog of RRL stars in the SMC from OGLE-II database (Soszyński et al. 2002, hereafter SZ02). The catalog contains B, V and I light curves of 58 RRc stars and 478 RRL stars located in the 11 areas close to the bar of the SMC in Johnson-Cousins photometric system. The target stars selected for the present analysis were passed through a multi-pass nonlinear fitting algorithm in IDL (Interactive Data Language) which is very efficient in removing the outliers from the data set. Points lying 2σ away from the fit are rejected from the data set so that the objects with well sampled and accurate light curves are available for the analysis. All the selected targets have evenly covered I band light curves with about 100 - 400 data points in I band with an internal accuracy of 0.03 - 0.13 mag in I band. The B and V light curves in the SZ02 catalog are of lower quality and have a limited number of data points (20-40). Therefore, we use only the I band data for estimation of the Fourier parameters. In Fig. 1(a) and (c) we show the typical phased light curve of a RRL and a RRc star in the database. The corresponding light curves with outliers $\geq 2\sigma$ removed are shown in panels (b) and (d) respectively.

3 FOURIER DECOMPOSITION OF THE LIGHT CURVES

Fourier decomposition technique is a powerful and robust technique for describing the shape of the photometric light curves of the RRL and other variable stars. The method has also been utilized for variable star classification (Deb & Singh 2009), finding the physical parameters of stars like absolute magnitude, metallicity, effective temperature, gravity, helium abundance etc. of RRL and other stars (Kovács &

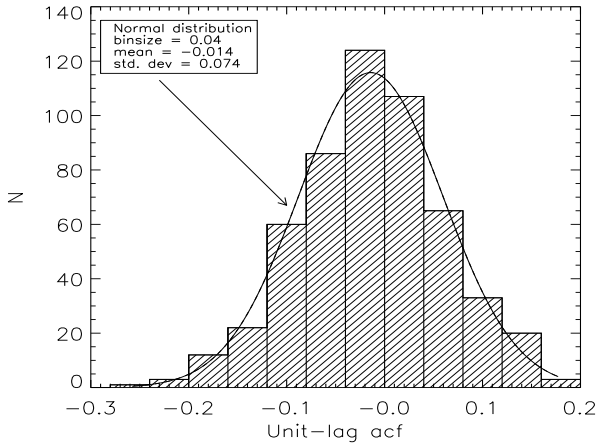


Figure 2. Histogram plot of unit-lag auto-correlation function for 536 SMC RRL stars in the OGLE database. The order of the fit is 4 and 5 respectively for the RRC and RRab stars.

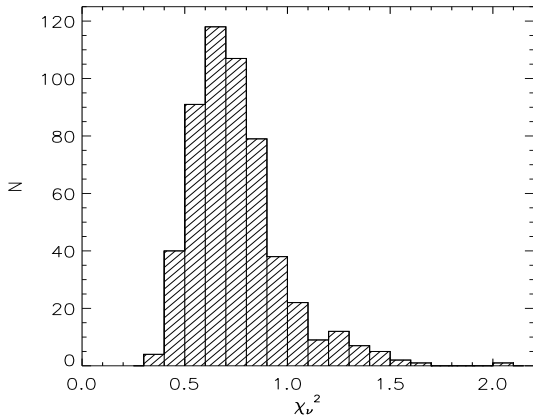


Figure 3. Histogram plot of χ^2 of 536 RRL stars selected from the database.

Kupi 2007 and references therein). The method in its modern form has been revived by Simon & Lee (1981) to describe the progression of Cepheid light curve with increasing period called Hertzsprung progression. They showed that the lower order Fourier parameters are able to completely describe the progression of Cepheid light curves. With theoretical light curves based on hydrodynamical models Simon & Lee (1981), Simon & Clement (1993, hereafter SC93), Clement & Rowe (2000) were able to derive various physical parameters of stars. On the other hand Kovács and his collaborators (Jurcsik & Kovács 1996, hereafter JK96, Kovács & Jurcsik 1996, Jurcsik 1998, Kovács 1998, Kovács & Kanbur 1998, Kovács & Walker 1999) were able to estimate astrophysical parameters by establishing empirical relationships between the Fourier parameters and the physical parameters of stars in the field. A number of studies have made use of these empirical relations to derive the physical parameters of the RRL stars. To list a few of these studies, Kaluzny et al. (2000) used these empirical relations to estimate physical parameters of 26 RRab and 16 RRC stars in M5, Peña et al. (2007) used these empirical relations to estimate physical pa-

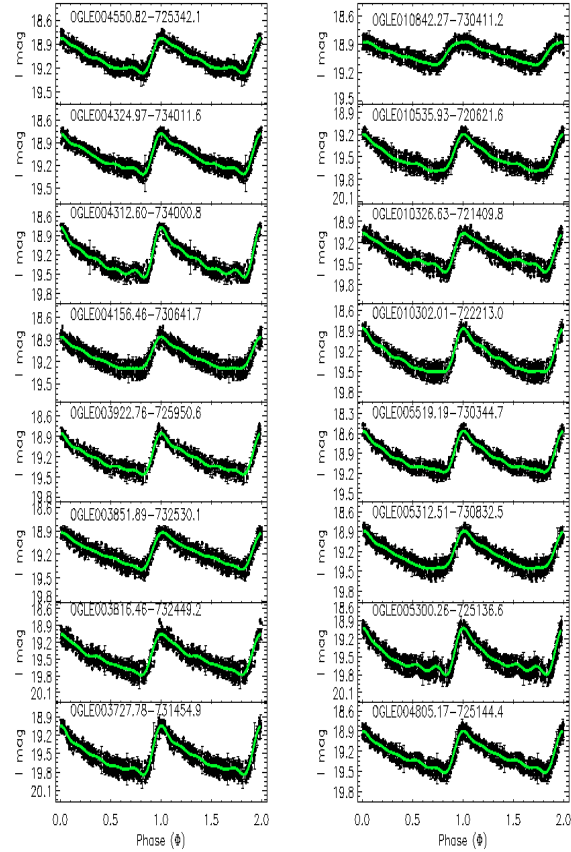


Figure 4. Fourier fitted light curves of a selection of RRab stars after pre-processing of outliers removal. The order of the fit to the light curve is 5. The solid lines show the Fourier fitted light curves.

rameters of 7 RRL stars in Bootes and Arellano et al. (2008) have determined parameters for few RRL variables in NGC 5466. There are a number of other studies that have made use of the Fourier coefficients to determine various parameters of astrophysical importance. Sandage (2004) studied the correlation of particular Fourier components of the light curves of RRab stars with metallicity discovered by Simon and later by Kovács and his co-workers. On the other hand, Morgan et al. (2006, 2007) have derived empirical relations for RRC stars connecting $[Fe/H]$, period (P) and Fourier parameter ϕ_{31} . In all the above studies, it has been seen that Fourier parameters can indeed be linked with global stellar parameters such as luminosity, mass, temperature, metallicity and radius. Most of the physical parameter estimations of stars require accurate calculation of Fourier parameters and any inaccuracies in the determination of Fourier parameters will reflect in the calculated physical parameters of the stars.

We computed Fourier decomposition coefficients for 536 RRL stars in the SMC for the I band photometric data. The observed magnitudes were fitted with a Fourier cosine series of the form

$$I(t) = A_0 + \sum_{i=1}^m A_i \cos(i\omega(t - t_0) + \phi_i), \quad (1)$$

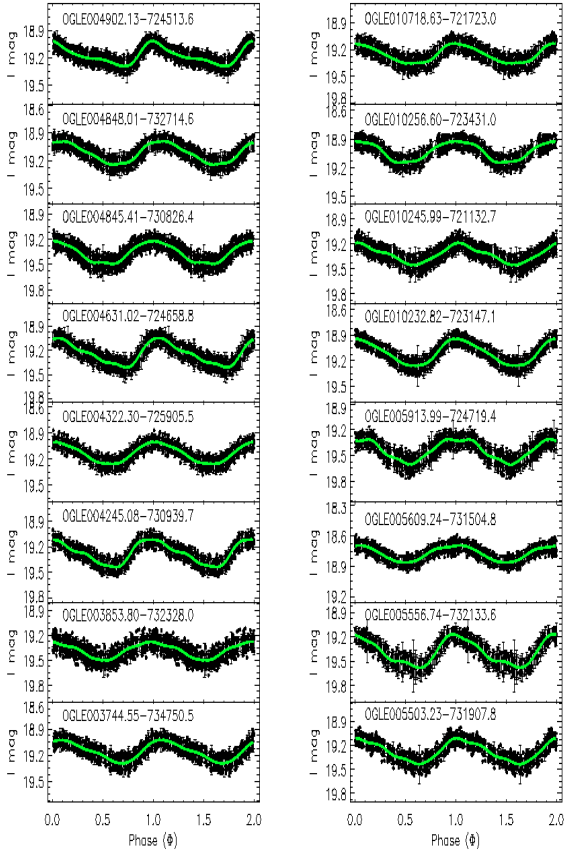


Figure 5. Fourier fitted light curves of a selection of RRc stars after removing the outliers. The order of the fit to the light curve is 4. The solid lines are the Fourier fitted light curves.

where $I(t)$ is the observed magnitude, A_0 is the mean magnitude, $\omega=2\pi/P$ is the angular frequency, P is the period of the star in days, t is the time of observation, t_0 is the epoch of maximum light, A_i and ϕ_i are the i th order Fourier coefficients and m is the order of the fit. Eqn. (1) has $2m + 1$ unknown parameters which require at least the same number of data points to solve for these parameters.

Since period is known from the database, the observation time can be folded into phase (Φ) as

$$\Phi = \frac{(t - t_0)}{P} - \text{Int} \left(\frac{(t - t_0)}{P} \right).$$

Here t_0 is the epoch of maximum light of the RRL light curves. The value of Φ is from 0 to 1, corresponding to a full cycle of pulsation and Int denotes the integer part of the quantity. Hence, Eqn. (1) can be written as (Schaltenbrand & Tammann 1971)

$$I(t) = A_0 + \sum_{i=1}^m A_i \cos[2\pi i \Phi(t) + \phi_i]. \quad (2)$$

The Fourier parameters are defined as

$$R_{i1} = \frac{A_i}{A_1}; \quad \phi_{i1} = \phi_i - i\phi_1,$$

where $i > 1$. The ϕ_{i1} values have been adjusted to lie be-

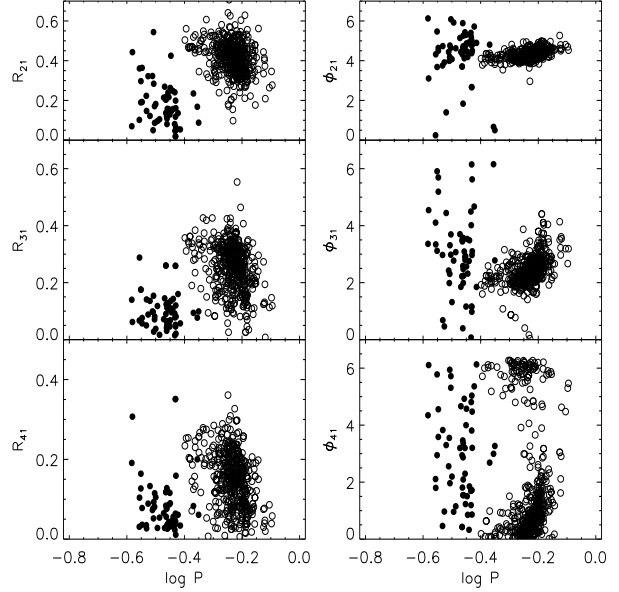


Figure 6. Fourier phase differences ϕ_{21} and ϕ_{31} as a function of $\log P$ for the I band data of 536 program stars. Open circles represent RRab stars and filled circles RRc stars.

tween 0 and 2π so that they are comparable to those available in the literature.

The optimal order of the fit (m) was chosen to be 4 for RRc stars and 5 for RRab stars by the calculation of unit-lag auto-correlation function (Fig. 2) and looking at the χ^2 value of the fit. A detailed discussion on the optimal order of the fit has been given in Deb & Singh (2009) which involves the calculation of unit-lag auto-correlation function using Baart's condition (Baart 1982, Petersen 1986). Increasing the order of the fit may reduce the χ^2 to some extent but this will underestimate the distribution. The fits to the phase-folded light curves were made using Levenberg-Marquardt (LM) algorithm which is based on χ^2 minimization method (Press et al. 1992). The reduced chi-square for the fit to the RRL light curves are nearly 1. The histogram plot of the χ^2_ν of the RRL stars is shown in Fig. 3, where ν is the degree of freedom of the fit which is defined as the number of data points minus the number of parameters used to fit the light curve data.

In Figs. 4 & 5 we show smoothed (outliers removed) Fourier fitted light curves for 16 randomly selected RRab and RRc stars respectively. Further, the Fourier parameters for all the stars computed from the I band data are given in Table 1 (for RRab) and Table 2 (for RRc). N_{obs} denotes the number of data points for each of the light curves retained for the analysis after removing the outliers. D_m is the deviation parameter for RRab stars and is discussed in Sec. (6.1). In Fig. 6 we plot the Fourier amplitude ratios R_{21} , R_{31} , R_{41} and phase differences ϕ_{21} , ϕ_{31} , ϕ_{41} versus $\log P$ for the RRL dataset.

4 ERRORS IN THE FOURIER PARAMETERS

The error in $x = f(u, v)$, where the standard errors in u 's and v 's are known from LM method, is given by

Table 1. Fourier parameters for 478 fundamental mode (RRab) SMC RRL variables in the OGLE database (I BAND DATA)

OGLE ID (1)	Period (2)	N _{obs} (3)	χ _ν ² (4)	σ _{fit} (5)	A _I (6)	A ₀ (7)	A ₁ (8)	R ₂₁ (9)	R ₃₁ (10)	R ₄₁ (11)	φ ₂₁ (12)	φ ₃₁ (13)	φ ₄₁ (14)	D _m (15)
004801.59-733021.5	0.399572	292	0.503	0.060	0.821	19.513	0.268	0.504	0.357	0.234	4.105	1.924	0.187	4.737
005300.26-725136.6	0.403584	306	0.716	0.058	0.786	19.519	0.257	0.561	0.311	0.253	3.785	1.602	5.713	3.860
003841.21-734422.9	0.410569	289	0.664	0.060	0.843	19.566	0.285	0.468	0.344	0.254	3.888	1.885	6.001	1.195
003727.78-731454.9	0.412698	286	0.815	0.060	0.799	19.540	0.276	0.463	0.336	0.204	4.116	2.060	0.093	0.356
005728.85-723454.6	0.416258	229	0.966	0.068	0.765	19.778	0.258	0.469	0.362	0.201	4.344	2.240	0.636	3.282
005728.85-723454.6	0.416260	229	0.966	0.068	0.765	19.778	0.258	0.469	0.362	0.201	4.344	2.240	0.636	3.282
005629.88-725213.0	0.422334	233	0.708	0.067	0.258	18.255	0.098	0.471	0.190	0.071	4.310	2.587	6.114	8.038
005026.32-732418.2	0.422681	314	1.024	0.057	0.630	19.598	0.222	0.469	0.338	0.145	4.164	1.970	6.021	1.151
004639.18-731324.7	0.424320	301	0.501	0.059	0.873	19.626	0.306	0.468	0.324	0.186	4.053	2.237	0.076	4.716
003816.46-732449.2	0.427897	291	1.273	0.060	0.734	19.469	0.262	0.519	0.279	0.125	4.367	2.351	0.986	4.522
005110.48-730750.0	0.431720	303	0.715	0.059	0.879	19.632	0.316	0.459	0.303	0.157	4.249	2.232	0.095	2.621
010134.33-725427.4	0.433496	291	1.001	0.060	0.645	19.413	0.234	0.440	0.235	0.133	4.165	1.999	5.184	6.134
010452.90-724025.9	0.433623	267	0.502	0.062	0.580	19.215	0.192	0.455	0.384	0.246	3.910	2.048	6.086	2.635
005719.62-725540.7	0.433862	254	0.627	0.064	0.747	19.536	0.256	0.530	0.283	0.230	4.080	1.775	0.061	7.359
005646.16-723452.2	0.445986	269	0.762	0.062	0.774	19.529	0.264	0.460	0.339	0.256	3.823	2.056	0.169	2.242
005957.83-730647.6	0.447303	256	0.686	0.064	0.784	19.465	0.277	0.447	0.297	0.217	3.913	2.161	0.240	3.408
005458.09-724948.9	0.447471	275	0.976	0.062	0.663	19.367	0.239	0.345	0.352	0.257	4.128	1.997	0.022	0.201
004758.98-732241.3	0.449794	299	0.520	0.059	0.764	19.818	0.253	0.484	0.333	0.267	4.059	2.227	0.090	3.250
010535.93-720621.6	0.453841	255	0.699	0.064	0.498	19.505	0.191	0.503	0.179	0.117	4.094	2.214	6.035	3.863
010516.55-722526.5	0.455958	256	0.599	0.064	0.756	19.522	0.255	0.498	0.315	0.204	4.267	2.523	0.391	4.913

Complete table is available in the electronic form.

Table 2. Fourier parameters for 58 overtone mode (RRc) SMC RRL variables in the OGLE database (I BAND DATA)

OGLE ID (1)	Period (2)	N _{obs} (3)	χ _ν ² (4)	σ _{fit} (5)	A _I (6)	A ₀ (7)	A ₄ (8)	R ₂₁ (9)	R ₃₁ (10)	R ₄₁ (11)	φ ₂₁ (12)	φ ₃₁ (13)	φ ₄₁ (14)
010220.67-723753.6	0.261244	281	0.599	0.061	0.202	19.611	0.018	0.066	0.142	0.193	6.051	3.361	4.371
010246.69-725030.1	0.262593	293	0.557	0.060	0.088	18.801	0.012	0.453	0.092	0.319	3.085	4.728	6.096
005609.24-731504.8	0.277551	265	0.784	0.063	0.173	18.774	0.003	0.103	0.066	0.032	0.250	4.089	1.937
005451.72-723850.4	0.277966	270	0.642	0.062	0.126	19.027	0.006	0.348	0.285	0.115	4.290	3.298	1.695
005115.64-724739.2	0.280936	313	0.743	0.058	0.171	19.161	0.011	0.192	0.177	0.128	5.505	3.101	2.957
003908.31-735426.8	0.281006	297	0.976	0.059	0.153	18.985	0.010	0.306	0.174	0.163	3.717	5.884	5.809
005601.43-724026.2	0.283717	271	0.713	0.062	0.296	19.584	0.009	0.363	0.075	0.078	4.639	5.659	3.513
005754.46-723248.2	0.283746	253	0.671	0.064	0.264	18.520	0.004	0.190	0.058	0.033	4.510	5.230	4.612
003706.77-730551.2	0.293459	292	0.800	0.060	0.141	19.198	0.002	0.236	0.071	0.030	3.767	2.998	0.587
010245.99-721132.7	0.294040	300	0.717	0.059	0.261	19.326	0.004	0.145	0.140	0.032	4.769	0.719	3.193
004744.89-725530.1	0.297777	306	0.664	0.058	0.243	19.185	0.010	0.311	0.091	0.088	3.865	0.441	0.843
004633.73-725253.8	0.302182	293	0.530	0.060	0.260	19.501	0.016	0.123	0.136	0.135	1.416	4.446	3.286
004631.02-724658.8	0.308220	300	0.459	0.059	0.362	19.241	0.011	0.322	0.096	0.071	4.444	2.469	2.491
003946.61-733332.6	0.309804	273	0.514	0.062	0.200	19.420	0.008	0.046	0.099	0.080	4.162	1.948	3.494
004902.13-724513.6	0.310884	314	0.599	0.057	0.282	19.180	0.005	0.541	0.157	0.053	4.196	2.315	6.005
004245.08-730939.7	0.311416	286	0.739	0.060	0.339	19.277	0.016	0.297	0.031	0.104	4.817	3.105	1.882
005503.23-731907.8	0.313536	278	1.096	0.061	0.321	19.275	0.011	0.171	0.076	0.075	4.616	2.970	5.392
005913.99-724719.4	0.313798	252	0.584	0.064	0.305	19.440	0.019	0.078	0.083	0.128	6.105	3.581	5.656
010249.92-720947.1	0.316409	277	0.518	0.061	0.271	19.379	0.014	0.173	0.039	0.110	4.034	1.202	2.223
004330.74-733416.0	0.320723	289	0.741	0.060	0.174	19.293	0.002	0.096	0.115	0.021	5.961	2.734	1.187

Complete table is available in the electronic form.

$$\sigma^2(x) = \sigma_u^2 \left(\frac{\partial x}{\partial u}\right)^2 + \sigma_v^2 \left(\frac{\partial x}{\partial v}\right)^2 + \dots + 2\sigma_{uv}^2 \left(\frac{\partial x}{\partial u}\right) \left(\frac{\partial x}{\partial v}\right). \quad (3)$$

In the case of a large number of observations Eqn. (3) can be reasonably approximated by

$$\sigma^2(x) = \sigma_u^2 \left(\frac{\partial x}{\partial u}\right)^2 + \sigma_v^2 \left(\frac{\partial x}{\partial v}\right)^2. \quad (4)$$

Therefore the errors in R_{i1} and φ_{i1} can be approximately written as

$$\sigma_{R_{i1}} = \frac{1}{A_{i1}^2} \sqrt{(\sigma_{A_{i1}}^2 A_{i1}^2 + \sigma_{A_{i1}}^2 A_{i1}^2)}, \quad (5)$$

$$\sigma_{\phi_{i1}} = \sqrt{\sigma_{\phi_{i1}}^2 + i^2 \sigma_{\phi_{i1}}^2}. \quad (6)$$

In Figs. 7 & 8 we plot the distribution of estimated errors in the quantities R₂₁, R₃₁, R₄₁ and φ₂₁, φ₃₁ and φ₄₁. As is quite obvious that the errors in φ₃₁ are larger than the errors in φ₂₁ because the amplitudes for the higher order coefficients are smaller and hence it is very difficult to derive their phase with better precision.

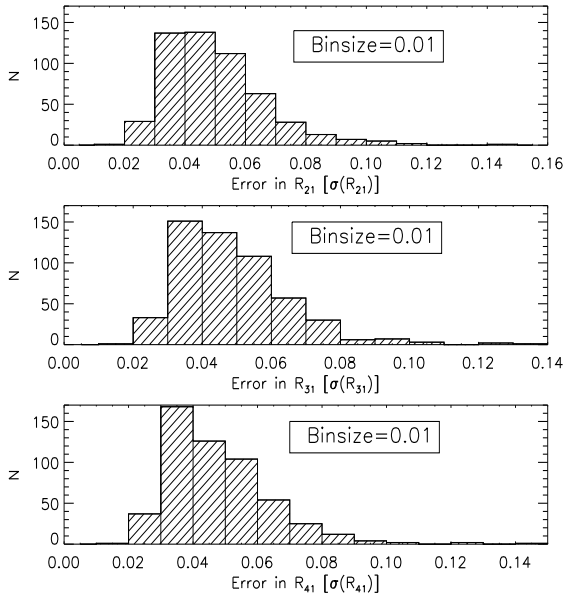


Figure 7. Histogram plot of the distribution of standard errors in R_{21} , R_{31} and R_{41} for the I band data.

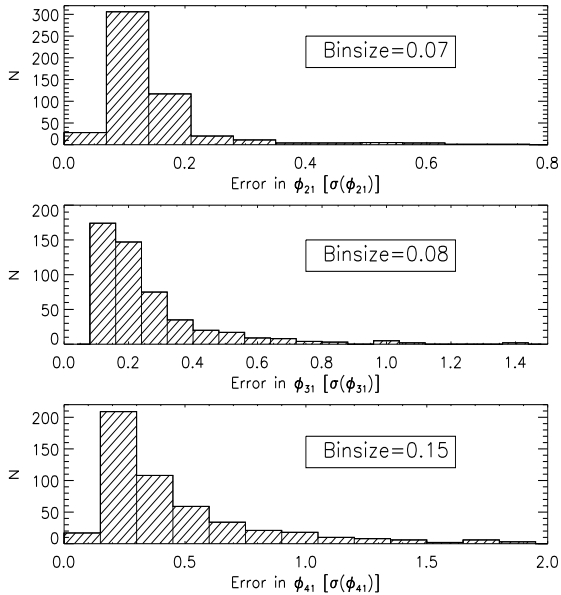


Figure 8. Histogram plot of the distribution of standard errors in ϕ_{21} , ϕ_{31} and ϕ_{41} for the I band data.

5 CALIBRATION OF THE OGLE SMC RRL DATASETS

5.1 Fourier parameters in V band

The Fourier coefficients of a particular light curve in different photometric bands are different. Nonlinear hydrodynamical models have been used by Dorfi & Feuchtinger (1999, hereafter DF99) to obtain UBVI light curves of RRL stars. They have computed the inter-relations of the Fourier parameters in V and I bands and compared them with those obtained by Morgan et al. (1998, hereafter MSB98) from observed light curves of metal poor globular cluster M68 by Walker

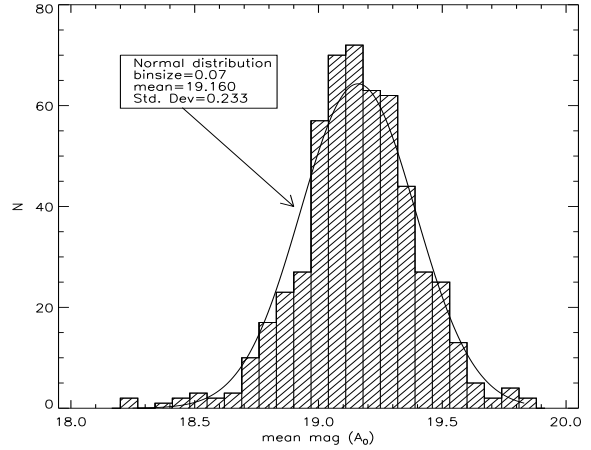


Figure 9. Histogram plot of magnitudes of 536 RRL stars. The solid line is the best fit normal distribution.

(1994, hereafter W94). However, only 8 RRab and 8 RRC stars from W94 were used for setting up the relations in MSB98. While the V-I inter-relations for amplitude ratios (R_{i1}) of DF99 showed good agreement with the empirical relations of MSB98, large deviations showed up in the relations of some of the phase differences (ϕ_{i1}) for two sets of models with $Z = 0.001$ and 0.0001 . DF99 concluded that no distinct metallicity effect could be followed from these results and emphasized the need for more model calculations covering a wide range of stellar parameters.

In order to check the reliability of the theoretical inter-relations of the phase parameters of DF99, we have calculated the Fourier phase parameters in the I and V bands from the highly accurate photometric light curves of selected RRab and RRC stars in globular cluster M3 from Benkó et al. (2006, hereafter B06) together with the data of 8 RRab and 8 RRC stars from W94. All the RRab stars free from Blazhko effect and RRC stars having good quality light curves were selected from B06 after visual inspection. We have used 29 RRab variables 1, 6, 9, 25, 27, 31, 32, 42, 53, 57, 58, 69, 84, 89, 93, 94, 100, 109, 135, 137, 139, 142, 144, 146, 148, 165, 167, 175, 222 of globular cluster M3 from B06 and 8 variables 2, 9, 10, 14, 22, 23, 25, 35 of globular cluster M68 from W94. In the case of RRC stars, 16 variables 21, 37, 75, 86, 88, 107, 126, 128, 131, 147, 152, 171, 177, 208, 213, 259 of globular cluster M3 from B06 and 8 variables 1, 6, 11, 13, 16, 18, 20, 24 of globular cluster M68 from W94 were used. We call this data set as B06+W94. In Fig. 10, we show the V-I inter-relations of the Fourier phase parameters ϕ_{21} , ϕ_{31} , ϕ_{41} for RRab and RRC stars respectively. Points lying above a threshold sigma (σ_{thres}) from the fit are rejected using multi-pass fitting algorithm in IDL. The threshold sigma level is chosen based on a reasonably high degree of correlation between the parameters in the I and V band so that the number of data points for the fit retained are significant. The mean difference of 0.61% in absolute magnitude, 0.23% in $\log(L/L_{\odot})$, 4.03% in $[\text{Fe}/\text{H}]$, 0.10% in effective temperature and 1.18% in mass will result when DF99 inter-relations are used.

The Fourier inter-relations of the phase parameters from the I band to the V band have the following form:

$$\phi_{i1}^{\text{V}} = \alpha + \beta \phi_{i1}^{\text{I}}. \quad (7)$$

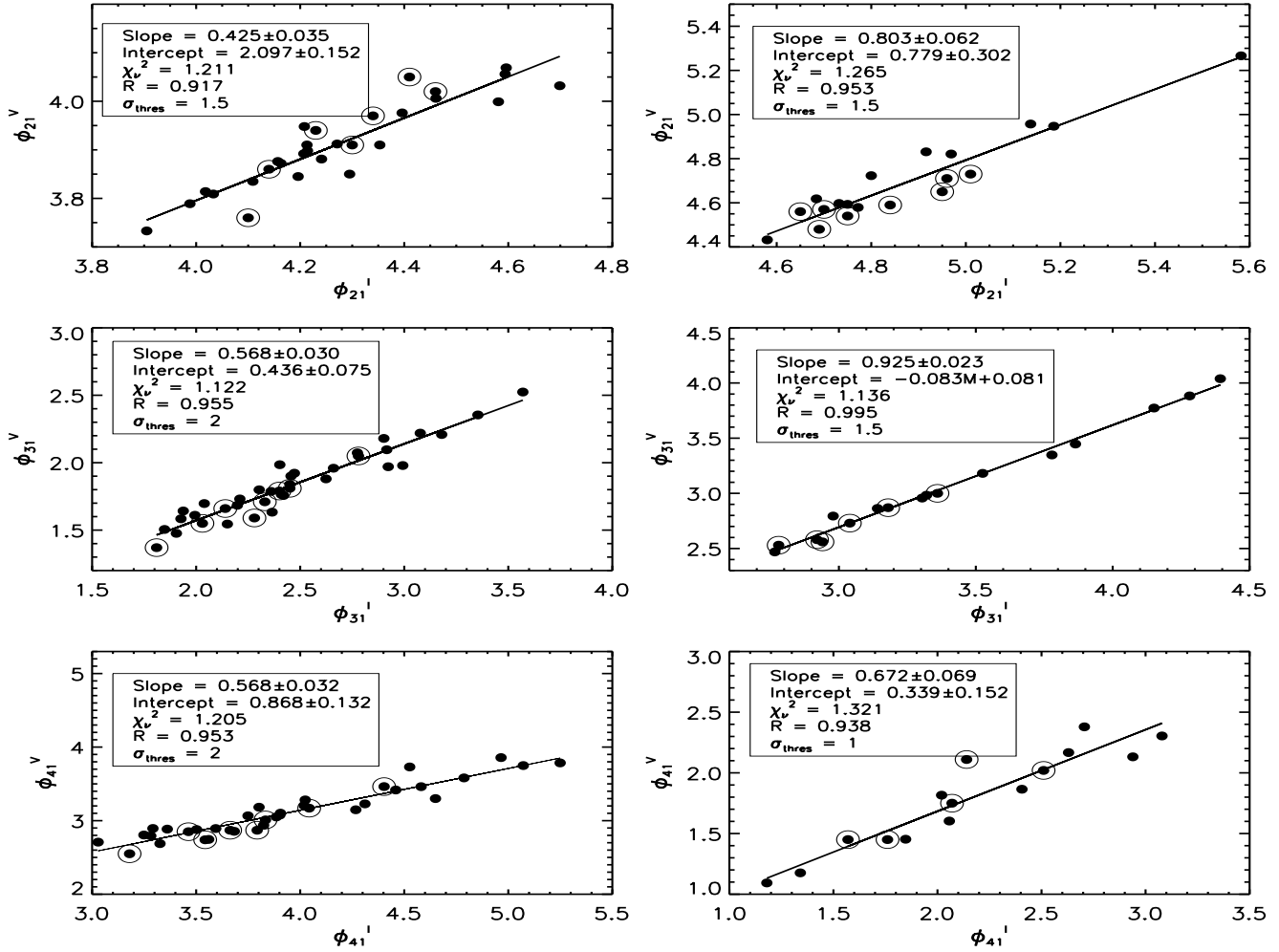


Figure 10. Observational inter-relations between V and I band Fourier phase parameters. The left and the right panels show the inter-relations for the RRab and RRC stars respectively. The solid line is the linear fit to the data. The inter-relations are based on the cosine series fit. Dots represent the data points from B06 and encircled dots from W94 .

Table 3. Coefficients of the Fourier inter-relations for RRab stars from DF99 and B06+W94 data.

Relation	DF99		B06+W94	
	α	β	α	β
$\phi_{21}^I \rightarrow \phi_{21}^V$	0.693	0.697	2.097 ± 0.152	0.425 ± 0.035
$\phi_{31}^I \rightarrow \phi_{31}^V$	-0.039	0.788	0.436 ± 0.075	0.568 ± 0.030
$\phi_{41}^I \rightarrow \phi_{41}^V$	-0.611	0.810	0.868 ± 0.132	0.568 ± 0.033

Table 4. Coefficients of the Fourier inter-relations for RRC stars from DF99 and B06+W94 data.

Relation	DF99		B06+W94	
	α	β	α	β
$\phi_{21}^I \rightarrow \phi_{21}^V$	0.144	0.930	0.779 ± 0.302	0.803 ± 0.062
$\phi_{31}^I \rightarrow \phi_{31}^V$	-0.249	0.995	-0.083 ± 0.081	0.925 ± 0.023
$\phi_{41}^I \rightarrow \phi_{41}^V$	-0.305	0.980	0.339 ± 0.153	0.672 ± 0.069

In Tables 3 and 4, we list the inter-relations obtained from the B06+W94 dataset for RRab and RRC stars. Also given are the theoretical inter-relations of DF99. In Fig. 10, we plot the I and V band Fourier parameters. In Fig. 11, we plot the theoretical inter-relations between the I and V band of DF99 and observational inter-relations obtained from the B06+W94 dataset.

To compute V band amplitude from I band amplitude

we again resort to the existing work in the literature. In Fig. 12 we plot V band amplitudes as functions of I band amplitudes for RRL stars in 4 globular clusters, M68 from Walker (1994), IC 4499 from Walker & Nemeč (1996), NGC 1851 from Walker (1998) and M3 from Benkő et al. (2006). Solid line denotes the linear relation as determined by a least square fit given by

$$A_V = 0.071 (\pm 0.019) + 1.500 (\pm 0.040) A_I. \quad (8)$$

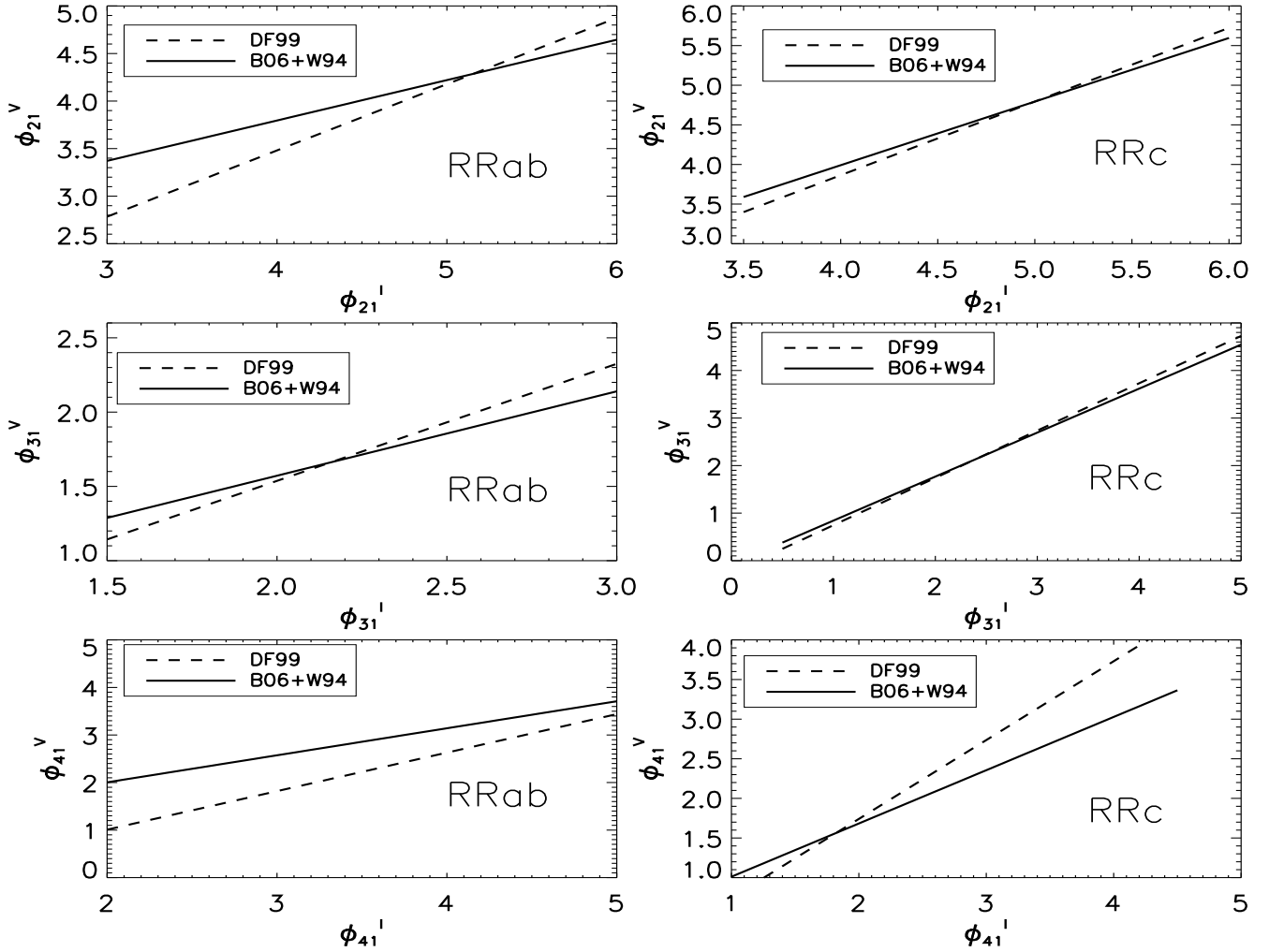


Figure 11. Theoretical inter-relations of DF99 between V and I band Fourier phase parameters in comparison with the observational relations calculated from the combined data set of B06 and W94 (B06+W94). The inter-relations are based on the cosine series fit.

5.2 Mean magnitudes in V band

Calibration to the standard V band magnitude is necessary for calculation of the distance scale. The mean magnitude was calculated for each object from its light curve. To transform the I band mean magnitude to the V band we used RRL light curves in the V and I band from the OGLE database itself. Typical errors in the V band magnitudes in OGLE are 0.02 - 0.07 mag. For RRab stars a linear least-square fit resulted in the following conversion relation :

$$A_0(V) = -0.691 (\pm 0.029) + 1.068 (\pm 0.002) A_0(I). \quad (9)$$

For the R R c stars the result of the linear least square fit is as follows:

$$A_0(V) = 3.733 (\pm 0.536) + 0.831 (\pm 0.028) A_0(I). \quad (10)$$

The fits of Eqns. (9) & (10) are shown in Fig. 14. Light curves having mean magnitude variation $\geq 2\sigma$ were discarded and V band magnitude thus determined. On the other hand, the absolute magnitude calculation of RRab stars required A_1 while R R c stars required A_4 in V band. We used V and I band Data from Walker (1994, 1998) for the A_4 V band cali-

bration and a linear regression analysis yielded the following relation

$$A_1(V) = -0.007 (\pm 0.001) + 1.686 (\pm 0.040) A_1(I), \quad (11)$$

for RRab stars and

$$A_4(V) = 0.001 (\pm 0.0007) + 1.056 (\pm 0.115) A_4(I), \quad (12)$$

for R R c stars. Following Saha & Hoessel (1990) and Sakai et al. (1999), the intensity weighted mean magnitudes and phase-weighted mean magnitudes are given by

$$m_{\text{int}} = -2.5 \log \sum_{i=1}^n \frac{1}{n} 10^{-0.4m_i}, \quad (13)$$

$$m_{\text{ph}} = -2.5 \log \sum_{i=1}^n 0.5(\phi_{i+1} - \phi_{i-1}) 10^{-0.4m_i}, \quad (14)$$

where n is the total number of observations, m_i and ϕ_i are the magnitude and phase of the i th observation respectively, in order of increasing phase. The intensity-weighted mean magnitude and phase-weighted mean magnitude in the V

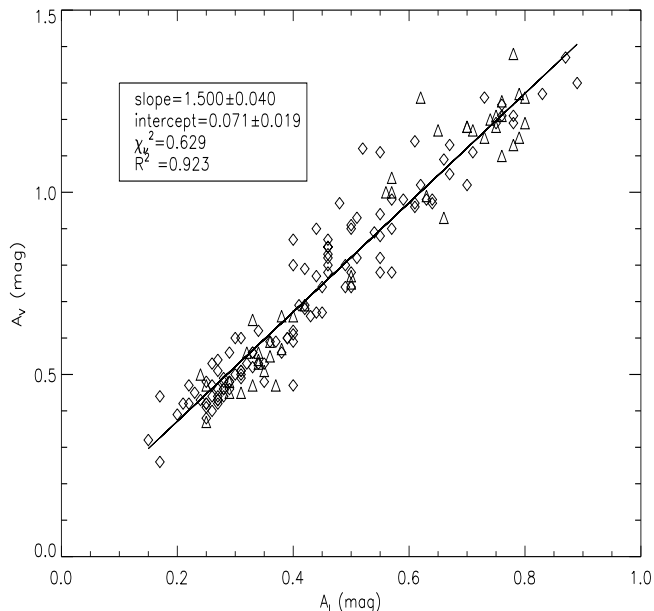


Figure 12. V band amplitudes as functions of I band amplitudes for RRL stars in 4 globular clusters. Solid line denotes the linear relation as determined by a least squares fit. The diamonds denote the observational data taken from Walker 1994 (M68), Walker & Nemeč 1996 (IC 4499) and Walker 1998 (NGC 1851). The triangles denote the amplitude relations determined by us from the published light curves from Benkó et al. (2006) (M3). The quadratic correlation coefficient is 0.923.

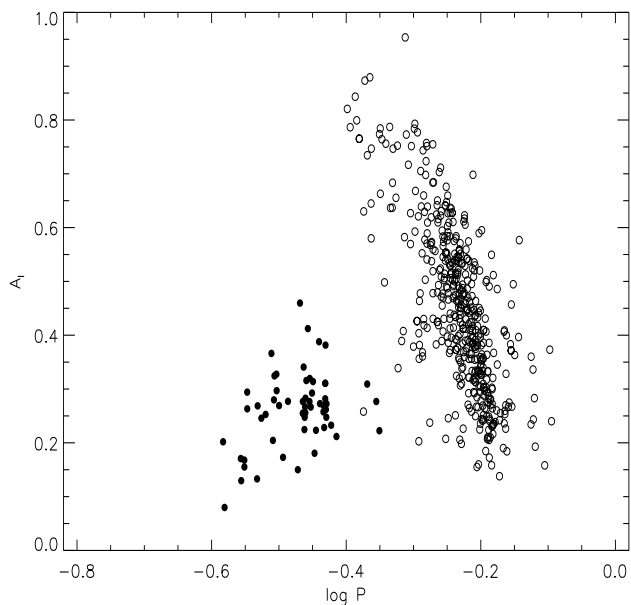


Figure 13. Period-amplitude diagram for all RRab (open circles) and RRc stars (filled circles).

band have been determined using a linear least square fit between the V and I band data resulting in the following conversion relations

$$m_{\text{int}}(V) = 0.862 (\pm 0.360) + 0.984 (\pm 0.019) m_{\text{int}}(I), \quad (15)$$

$$m_{\text{ph}}(V) = 0.471 (\pm 0.320) + 1.009 (\pm 0.021) m_{\text{ph}}(I), \quad (16)$$

for RRab stars, and

$$m_{\text{int}}(V) = 3.093 (\pm 0.867) + 0.863 (\pm 0.045) m_{\text{int}}(I), \quad (17)$$

$$m_{\text{ph}}(V) = 5.900 (\pm 0.893) + 0.733 (\pm 0.045) m_{\text{ph}}(I), \quad (18)$$

for RRc stars.

6 PHYSICAL PARAMETER EXTRACTION

6.1 RRab stars

Using a set of 81 RRab stars, JK96 derived an empirical relation between the Fourier decomposition parameter ϕ_{31} , period (P) and metallicity [Fe/H] given by

$$[\text{Fe}/\text{H}] = -5.038 - 5.394 P + 1.345 \phi_{31}. \quad (19)$$

The Fourier parameters in the above relation were obtained for a sine Fourier series fit. Care has to be taken that the RRab stars to which this equation is applied follow the light curve systematics defined by calibrating the sample of JK96. This can be ensured if the light curve in question satisfies a certain compatibility criterion. The various parameters of the calibrating data set obey well-defined correlations (see Table 6 of JK96). Deviation of a light curve from the calibrating characteristics is quantified via the deviation parameter D_F defined as

$$D_F = \frac{F_{\text{obs}} - F_{\text{calc}}}{\sigma_F},$$

where F_{obs} is the observed value of a given Fourier parameter, σ_F is the corresponding deviations of various correlations. If the maximum value of D_F of each parameter is less than 3, then each light curve satisfies the compatibility condition. This maximum value of D_m represents a quality test on the regular behaviour of the shape of the light curve. But when the test is applied to the RRab stars of OGLE SMC RR Lyrae stars, some of the stars did not pass this criterion even though the shapes of the light curve are ‘normal looking’. One of the possible reasons is that the OGLE SMC RRL light curves are constructed from the observation in the I band but not in the V band on which the deviation parameter is defined. We have noticed that for the deviation parameter up to a value of $D_m = 5$, the shapes of the RRab light curves are normal. This value of D_m is used as a cutoff limit for the selection of clean samples of RRab stars for analysis. The deviation parameter of individual RRab light curves of the OGLE data has been calculated and is given in the last column of Table 1. Cacciari et al. (2005) have also adopted this slightly relaxed criterion to improve the statistics after they verified that this does not lead to any significant difference in the resulting physical parameters. For the RRab analysis, we apply various empirical relations from the literature to all our target stars only when $D_m \leq 5$. After implementing this compatibility test we have found that 355 RRab stars out of 478 are now available for further analysis. This means that our sample of RRab stars now contains 355 RRab stars that have ‘normal looking’ light curve shapes. It is also seen that the maximum contribution to the deviation parameter comes from the deviation in ϕ_{31} .

The intrinsic colors as derived from the Fourier parameters of the RRab stars can be used to estimate the temperature of these stars. These color indices as defined by Jurcsik

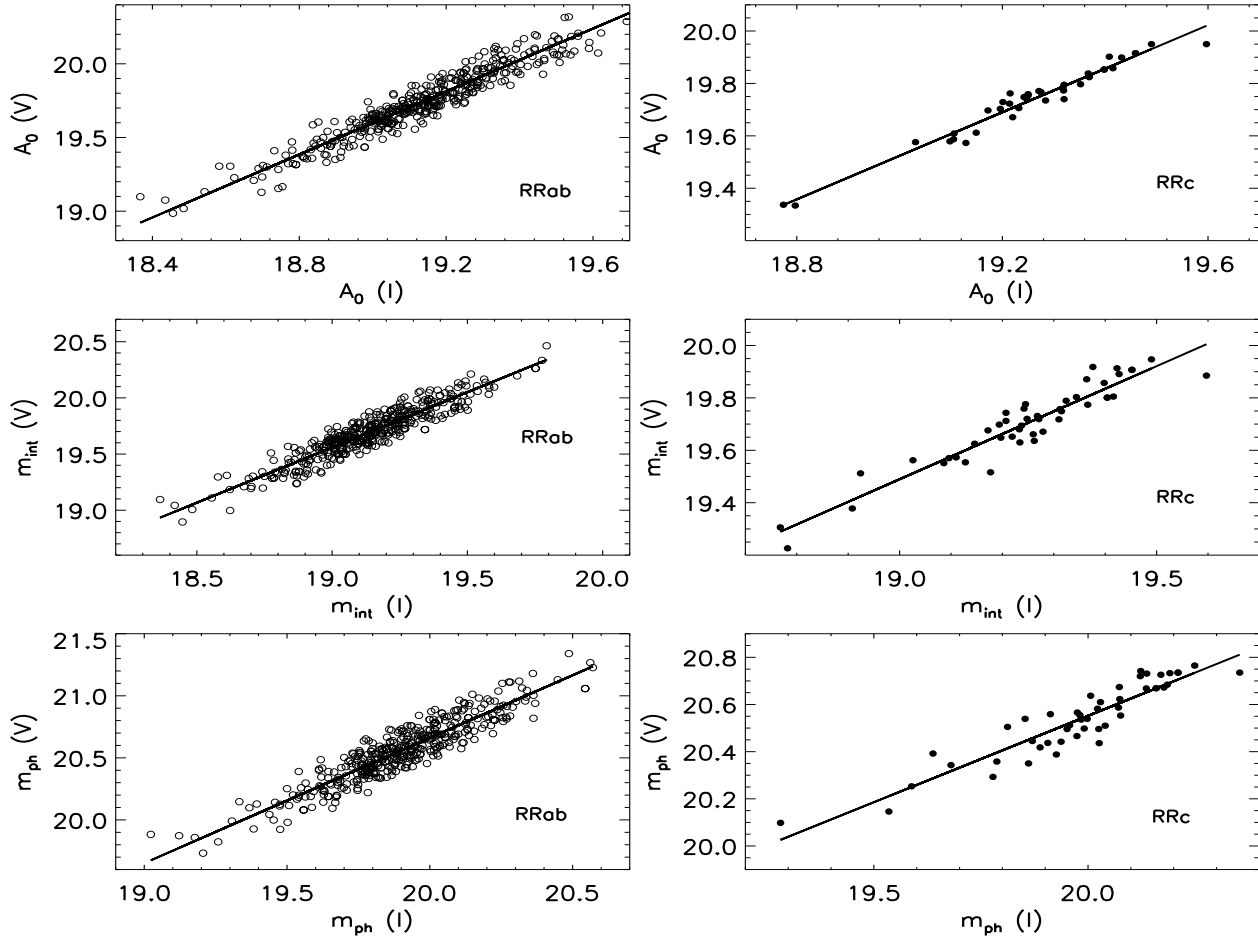


Figure 14. Mean magnitude V band calibration for RRab stars (open circles) and RRc stars (filled circles). Top panels show fits represented by Eqns. (9) & (10). The lower panels show mean magnitude calibration using both V and I band data available for 465 RRab and 55 RRc stars in SZ02.

(1998) are the differences of the magnitude-averaged absolute brightness. The intrinsic color relations is of the form

$$(B - V) = 0.308 + 0.163 P - 0.187 A_1. \quad (20)$$

The above relation can be used to calculate the effective temperature

$$\log T_{\text{eff}} (B - V) = 3.930 - 0.322 (B - V) + 0.007 [\text{Fe}/\text{H}]. \quad (21)$$

The relation between the absolute magnitudes and the Fourier parameters is given by the following relations

$$M_V = 1.221 - 1.396 P - 0.477 A_1 + 0.103 \phi_{31}. \quad (22)$$

Eqn. (20) is from Jurcsik (1998) and Eqn. (21) is taken from Kovács & Walker (2001). Eqn. (22), taken from Kovács (1998) is based on the relation between the intensity-averaged M_V and the V band Fourier parameters. On the other hand on a different absolute scale, Jurcsik (1998) derived a relation for the mass of the RRab stars as follows

$$\begin{aligned} \log (M/M_{\odot}) &= 20.884 - 1.754 \log P + 1.477 \\ \log (L/L_{\odot}) &= 6.272 \log T_{\text{eff}} + 0.0367 [\text{Fe}/\text{H}]. \end{aligned} \quad (23)$$

The Fourier coefficients in the above equations are based on a sine series fit. But the coefficients in the present

analysis (Table 1) are calculated for a cosine series fit. Therefore, to put the coefficient ϕ_{31} on to the appropriate system, we add 3.145 to ϕ_{31} in Table 1. In Table 5 we list various physical parameters computed from the above empirical relations for 335 RRab stars with regular light curves with $D_m \leq 5$. Mean error in the Fourier phase parameter ϕ_{31} for 335 RRab stars is ~ 0.19 . This should result in an uncertainty of ~ 0.25 dex in $[\text{Fe}/\text{H}]$, ~ 0.02 mag in the absolute magnitude, ~ 12 K in temperature, $\sim 0.01 M_{\odot}$ in mass.

6.2 RRc stars

For the RRc stars, we have only retained stars for which the error in ϕ_{31} is less than 0.5. It is generally not desirable to have error larger than 0.2 (Kaluzny et al. 1998). Since the RRc stars in the SMC are fainter and have lower amplitudes, good data for such sources are simply not available at present. Imposing the criterion of $\sigma_{\phi_{31}} < 0.3$ leaves us with only 3 RRc stars to be used for further analysis. To increase the statistics without significant loss of accuracy, we have chosen $\sigma_{\phi_{31}} < 0.5$ which allows us to analyse 17 RRc stars.

Through Hydrodynamical pulsation models, SC93 for-

mulated the following relationships for Luminosity, mass and helium abundance (Y) of RRc stars :

$$\log(L/L_{\odot}) = 1.04 \log P - 0.058 \phi_{31} + 2.41, \quad (24)$$

$$\log(M/M_{\odot}) = 0.52 \log P - 0.11 \phi_{31} + 0.39, \quad (25)$$

$$\log(T_{\text{eff}}) = 3.7746 - 0.1452 \log P + 0.0056 \phi_{31}. \quad (26)$$

$$\log Y = -20.26 + 4.935 \log(T_{\text{eff}}) - 0.2638 \log(M/M_{\odot}) + 0.3318 \log(L/L_{\odot}). \quad (27)$$

The rms error to the fit in Eqn. (24) is 0.025.

Another alternative to Eqn. (24) is the expression for the intensity averaged absolute magnitude proposed by Kovács (1998, hereafter K98) based on observations of RRc variables in eight different stellar systems:

$$M_V = 1.261 - 0.961 P - 0.044 \phi_{21} - 4.447 A_4, \quad (28)$$

with an rms of 0.042. Kovács derived this formula from the light curves of 106 RRc stars, mainly from Sculptor and M68 and calibrated the zero point from the Baade-Wesselink luminosity scale of Clementini et al. (1995). The phase difference ϕ_{21} in Eqn. (28) is based on a sine series fit. Therefore, 1.571 is subtracted from ϕ_{21} values in Table 2, which are based on a cosine series fit.

Following Lázaro et al. (2006), we have calculated the luminosities of SMC RRc stars from Eqn. (24) as well as from Eqn. (28). The results are plotted in Fig. 15. Luminosities calculated using SC93 relation (Eqn. (24)) are larger than those estimated by the K98 relation (Eqn. (28)) and the difference may be attributed to different scaling (zero points) of the two relations. The zero point of the luminosity scale of RRc stars is still a matter of controversy (Cacciari et al. 2005, Nemeč 2004, Lázaro et al. 2006). Some problems with the Simon's calibration for the RRc stars were also noted by Catelan (2004) who concluded that SC93's relations for L and M cannot both be simultaneously valid. Eqns. of SC93 (Eqns. (24) & (25)) yield

$$\log P = -2.877 + 1.305 \log(L/L_{\odot}) - 0.688 \log(M/M_{\odot}), \quad (29)$$

The above relation lacks a temperature term which should be present according to the period-density relation (Catelan 2004). This is true and remains an unresolved theoretical issue.

The empirical relation for metallicity in terms of the Fourier decomposition parameter ϕ_{31} was derived by Morgan et al. (2007) by considering a large number of stars in different globular clusters which have the V band Fourier coefficients available in the literature and the sources of metallicities available for these cluster members. Using the metallicity scales of Zinn & West (1984) and Carretta & Gratton (1997), they obtained the following two empirical relations for RRc stars respectively

$$[\text{Fe}/\text{H}] = 52.466 P^2 - 30.075 P + 0.131 \phi_{31}^2 + 0.982 \phi_{31} - 4.198 P \phi_{31} + 2.424, \quad (30)$$

which has a sample standard deviation of 0.145 dex, and

$$[\text{Fe}/\text{H}] = 0.034 \phi_{31}^2 + 0.196 \phi_{31} - 8.507 P + 0.367, \quad (31)$$

which has a sample standard deviation of 0.142 dex. We have used Eqn. (31) for the calculation of $[\text{Fe}/\text{H}]$.

The temperatures determined using Eqn. (26) are found to be overestimated for some of the RRc stars. Cacciari et al. (2005) also used Eqn. (26) and found a similar trend for temperature estimates of RRc stars of globular cluster M3 when compared with temperatures derived by Sekiguchi & Fukugita (2000) from the B-V Colors. Temperature differences as large as 500 K have been found for some of the RRc stars. Therefore, the temperature of RRc stars as determined from Fourier coefficients need to be re-examined. The inaccuracy of the empirical relations connecting the effective temperature, ϕ_{31} term and the period is also reflected in the calculation of the radius of RRc stars. We show ahead that the radii of RRc stars determined from the Fourier decomposition technique differ largely from those determined from the theoretical period-radius-metallicity relation of Marconi et al. (2005). On the other hand, for RRab stars there is a well-matched similarity between the radii determined from the Fourier decomposition technique and from the more fundamental relations used by Marconi et al. (2005). Therefore, the empirical relations derived for the RRab stars seem to be accurate, whereas the physical parameter estimation using the empirical relations derived for the RRc stars may be unreliable. In Table 6, we list the various physical parameters computed from the above empirical relations for the RRc stars with $\sigma_{\phi_{31}} < 0.5$.

Mean error in the Fourier phase parameter ϕ_{31} for 17 RRc stars is ~ 0.396 . This will result in an uncertainty of ~ 0.14 dex in $[\text{Fe}/\text{H}]$, ~ 0.02 in $\log(L/L_{\odot})$, ~ 16 K in temperature and $\sim 0.18 M_{\odot}$ in mass.

6.3 HR Diagram

An H-R diagram of the SMC RRLs stars is plotted in Fig. 15 along with the theoretical blue and red edges of the instability strip. The RRc stars are represented by solid circles whereas the RRab stars are represented by open circles. Also shown are the blue and red edges of the instability strip of Fundamental (RRab) and first-overtone (RRc) variables derived from the theoretical convective pulsation models of Bono, Caputo & Marconi (1995). It can be easily seen that all the RRab and RRc stars lie well within their instability strips. Although the RRc stars lie inside the instability strip, the empirical relations overestimate the temperatures of these stars.

6.4 Gravity for RRab and RRc stars

From the global physical parameters like mass, luminosity and temperature, the gravity can be calculated from the following equation (cf. Cacciari et al. 2005)

$$\log g = -10.607 + \log(M/M_{\odot}) - \log(L/L_{\odot}) + 4 \log T_{\text{eff}} \quad (32)$$

6.5 Radii of RRLs

The radii of the RRL can be obtained once we know the temperature and the luminosity of the RRLs stars using the Stefan-Boltzmann law. Marconi et al. (2005) have recently given a new theoretical period-radius-metallicity relation for

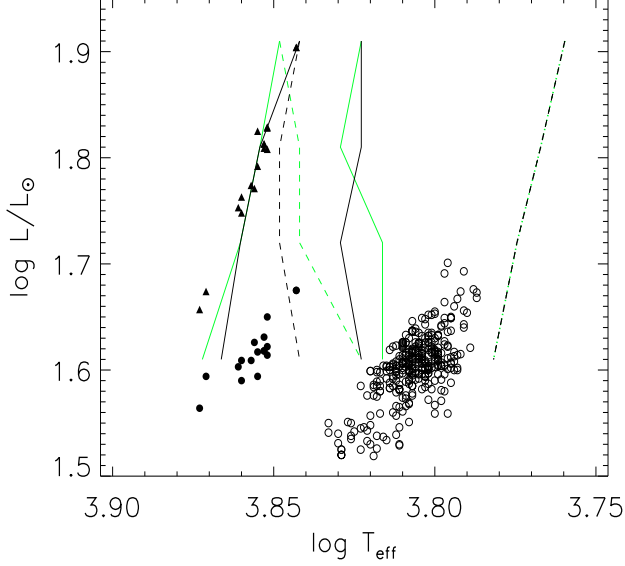


Figure 15. H-R diagram of 335 RRab and 17 RRc stars and the theoretical pulsational blue and red edges of the instability strip from Bono et al. (1995). Open circles represent RRab stars, solid circles represent RRc stars with $\log(L/L_{\odot})$ calculated from Eqn. (28) and filled upper triangles RRc stars with $\log(L/L_{\odot})$ calculated from Eqn. (24). The green solid and dashed lines show the boundaries of the instability strip for RRc and RRab stars respectively for mass $0.75M_{\odot}$ and the black solid and dashed lines show the boundaries of the instability strip for RRc and RRab stars respectively for mass $0.65M_{\odot}$.

the RR Lyraes based on detailed and homogeneous set of nonlinear models with a wide range of stellar masses and chemical compositions. We show how the radii obtained by the Fourier decomposition method compare to the radii obtained from the period-radius-luminosity (PRZ) relation of Marconi et al. (2005). For the sake of completeness, their PRZ relations are given as follows:

$$\log R = 0.774(\pm 0.009) + 0.580(\pm 0.007) \log P - 0.035(\pm 0.001) \log Z, \quad (33)$$

for RRab stars with $\sigma = 0.008$.

$$\log R = 0.883(\pm 0.004) + 0.621(\pm 0.004) \log P - 0.0302(\pm 0.001) \log Z, \quad (34)$$

for RRc stars with $\sigma = 0.004$. $\log Z$ can be calculated from the relation

$$\log Z = [\text{Fe}/\text{H}] - 1.70 + \log(0.638f + 0.362), \quad (35)$$

where f is an α -enhancement factor with respect to iron (Salaris, Chieffi & Straniero 1993). We take $f = 1$. In Fig. 16, we compare our determinations of the radii using the Fourier decomposition technique (FD) with those obtained by Marconi et al. (2005) empirical relations (Mar). In case of the radius determinations of RRc stars by the FD method, the SC93's equations for $\log L$ and $\log T$ are used. It can be seen that the radii obtained by the two different methods are quite consistent for RRab stars. The solid line in Fig. 16

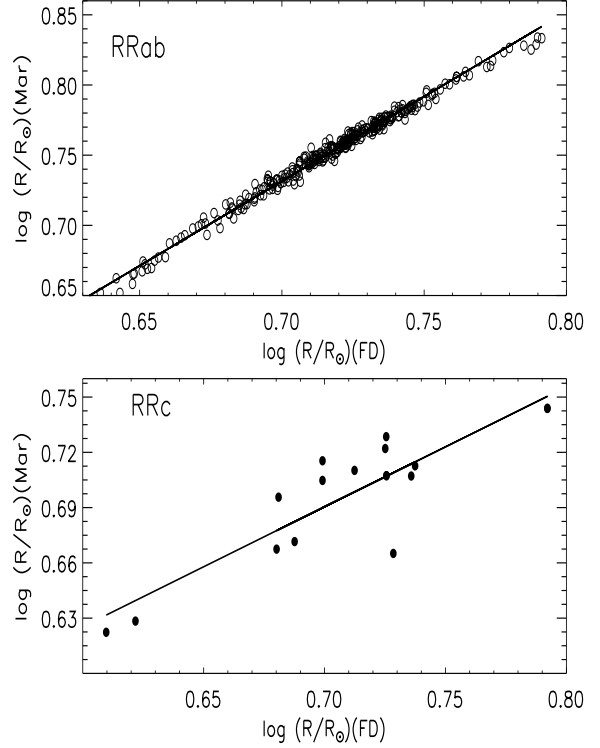


Figure 16. Radii obtained from the empirical relation of Marconi et al. (2005) are plotted versus the radii determined from the Fourier decomposition (FD) method. For RRab (open circles) stars in the upper panel the linear regression analysis yields : $\log(R/R_{\odot})(\text{Mar}) = -0.112(\pm 0.005) + 1.206(\pm 0.007) \log(R/R_{\odot})(\text{FD})$ and for the RRc stars (filled circles) in the lower panel the linear regression analysis yields: $\log(R/R_{\odot})(\text{Mar}) = 0.235(\pm 0.064) + 0.651(\pm 0.090) \log(R/R_{\odot})(\text{FD})$.

represents the best least square fit. The correlation coefficient between the two radii determinations for the RRab stars are 0.994, whereas for the RRc stars (lower panel of Fig. 16), the correlation coefficient is 0.880. This suggests that the radii determinations by the two independent methods are strongly correlated for the RRab stars, whereas this is not the case for the RRc stars.

7 DISTANCE TO THE SMC

We use mean magnitude $A_0(V)$, intensity-weighted mean magnitude and phase weighted mean magnitude separately to derive an independent distance modulus to the SMC. The distance modulus for each star is calculated from their values of mean magnitudes and M_V derived from the Fourier parameters. Assuming the reddening estimates of the eleven SMC fields of SZ02 to be accurate, we take average of the reddening values of these fields as the true estimates of $E(B-V)$. Following SZ02 we take the interstellar extinction as $A_V = 3.24E(B-V)$. This value of A_V has been used to estimate the reddening free distance modulus of SMC. Using 335 RRab and 17 RRc stars we find the mean distance moduli of SMC to be 18.89 ± 0.01 mag, 18.87 ± 0.03 mag and 18.87 ± 0.02 mag from the mean magnitude, intensity-weighted mean magnitude and phase-weighted mean magnitude respectively for all the 352 RRL stars. The uncertainty is the

standard deviation of the mean from the individual stars. The mean distance modulus so determined are consistent with the earlier values of 19.05 ± 0.017 (Kovács et al. 2000), 18.89 ± 0.4 (Harries et al. 2003) and 18.91 ± 0.1 (Hilditch et al. 2005).

8 SUMMARY & CONCLUSIONS

In this paper we have derived the physical parameters of 352 RR Lyrae stars (335 RRab and 17 RRc) of the SMC from OGLE-II I band database using the Fourier decomposition of their light curves. The stars were selected based on the quality of their light curves. I band Fourier coefficients have been converted to V band using the interrelations obtained from the observational data of B06 and W94. Using the Fourier decomposition method, we find the mean physical parameters: $[\text{Fe}/\text{H}] = -1.56 \pm 0.25$, $M = 0.55 \pm 0.01 M_{\odot}$, $T_{\text{eff}} = 6404 \pm 12 \text{ K}$, $\log L = 1.60 \pm 0.01 L_{\odot}$ and $M_V = 0.78 \pm 0.02$ for 335 RRab variables and $[\text{Fe}/\text{H}] = -1.90 \pm 0.13$, $M = 0.82 \pm 0.18 M_{\odot}$, $T_{\text{eff}} = 7177 \pm 16 \text{ K}$, $\log L = 1.62 \pm 0.02 L_{\odot}$ and $M_V = 0.76 \pm 0.05$ for 17 RRc stars. Mean distance modulus to the SMC was calculated from the 352 light curves by using mean magnitude, intensity weighted mean magnitude and phase weighted mean magnitude. The values of the distance modulus are found to be in good agreement with independent studies. Locations of the RRL stars in the H-R diagram clearly show that the estimates of the parameters determined from the Fourier decomposition method are consistent with the theoretical blue and red edges of the instability strip calculated by Bono et al. (1995). The calculations of the radii of the RRLs by using the Fourier decomposition technique are in agreement with the theoretical period-radius-metallicity relations of Marconi et al. (2005) obtained from a completely different approach of non-linear convective modelling.

ACKNOWLEDGMENTS

SD thanks CSIR, Govt. of India for a Senior Research Fellowship. HPS is grateful to CRAL-Observatoire de Lyon for an Invited Professorship. Authors thank the reviewer Dr. Horace Smith for many useful comments and suggestions which improved the presentation of the paper.

REFERENCES

Arellano Ferro, A., Rojas López, V., Giridhar, S., Bramich, D. M. 2008, MNRAS, 384, 1444
 Baart, M. L., 1982, IMA J. Num. Analysis, 2, 241
 Benkő, J. M., Bakos, G. Á, Nuspl, J. 2006, MNRAS, 372, 1657 (B06)
 Bono, G., Caputo, F., Marconi, M. 1995, AJ, 110, 2365
 Brown, T. M., Ferguson, H., Smith, E., Kimble, R. A., Sweigart, A. V., Renzini, A, Rich, R. M. 2004, AJ, 127, 2738
 Cacciari, C., Corwin, T. M., Carney, B. E., 2005, AJ, 129, 267
 Carretta, E., Gratton, R. G., 1997, A&AS, 121, 95
 Catelan, M., 2004, ASPC, 310, 113
 Clement, C. M., Rowe, J., 2000, AJ, 120, 2579

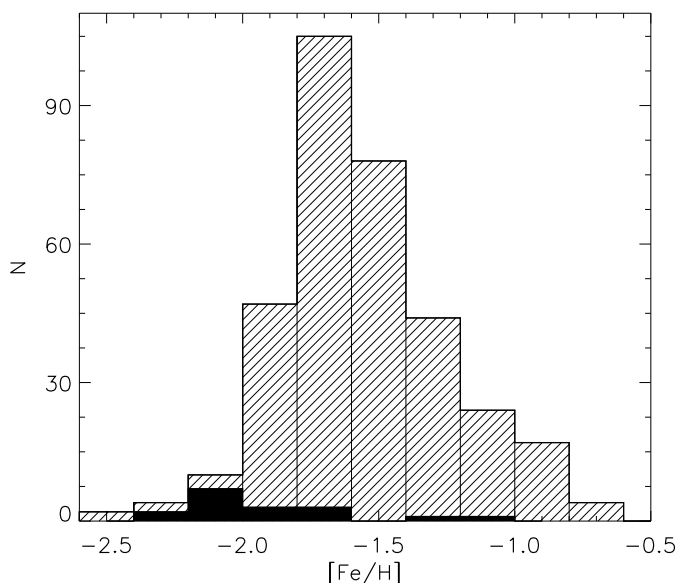


Figure 17. Histogram of the metallicity of the RRLs used for the analysis. The partially filled histogram shows the metallicity distribution of the 335 RRab stars, whereas the fully filled histogram shows the metallicity distribution of the 17 RRc stars.

Clementini, G., Carretta, E., Gratton, R., Merighi, R., Mould, J. R., & McCarthy, J. K., 1995, AJ, 110, 2319
 Clementini, G., Federici, L., Corsi, C., Cacciari, C., Bellazzini, M., Smith, H. A., 2001, ApJ, 559, L109
 Clementini, G., Bragaglia, A., Di Fabrizio, L., Maio, M. et al., 2002, ASPC, 259, 124
 Deb, S., Singh, H. P., 2009, A&A (in press); arXiv:0903.3500v3
 Dorfi, E. A., Feuchtinger, M. U., 1999, A&A, 348, 815 (DF99)
 Dolphin, A. E., Saha, A., Olszewski, E. W., Thim, F., Skillman, E. D., Gallagher, J. S., Hoessel, J., 2004, AJ, 127, 875
 Greco, C., Clementini, G., Catelan, Márcio, Held, E., V. et al., 2007, ApJ, 670, 332
 Harries, T. J., Hilditch, R. W., Howrath, I. D., 2003, MNRAS, 339, 157
 Hilditch, R. W., Howrath, I. D, Harries, T. J., 2005, MNRAS, 357, 304
 Jurcsik, J., Kovács, G., 1996, A&A, 312, 111 (JK96)
 Jurcsik, J., 1998, A&A, 333, 571
 Kaluzny, J., Hilditch, R. W., Clement, C., Rucinski, S. M., 1998, MNRAS, 296, 347
 Kaluzny, J., Olech, A., Thompson, I., Pych, W., Krzeminski, W., Schwarzenberg-Czerny, A., 2000, A&AS, 143, 215
 Kovács, G., Jurcsik, J., 1996, ApJ, 466, L17
 Kovács, G., Jurcsik, J., 1997, A&A, 322, 218
 Kovács, G., 1998, Mem. Soc. Astron. Italiana, 69, 49 (K98)
 Kovács, G., 2000, A&A, 360, L1
 Kovács, G., Walker, A. R., 1999, ApJ, 512, 271
 Kovács, G., Walker, A. R., 2001, A&A, 374, 264
 Kovács, G. 2005, A&A, 438, 227
 Kovács, G., Kanbur, S. M. 1998, MNRAS, 295, 834

Table 5. Physical parameters extracted from Fourier coefficients for 335 RRab variables. Errors represent the uncertainties in the Fourier parameters.

OGLE ID (1)	M_V (2)	$\log(L/L_\odot)$ (3)	[Fe/H] (4)	T_{eff} (5)	M/M_\odot (6)	$\log g$ (7)	R/R_\odot (FD) (8)	R/R_\odot (Mar) (9)
004801.59-733021.5	0.93± 0.02	1.53± 0.01	-0.91± 0.19	6751± 9	0.61± 0.01	2.97± 0.02	4.27± 0.02	4.31± 0.03
005300.26-725136.6	0.92± 0.02	1.54± 0.01	-1.18± 0.19	6702± 9	0.64± 0.01	2.97± 0.02	4.40± 0.02	4.43± 0.03
003841.21-734422.9	0.90± 0.01	1.54± 0.01	-1.00± 0.18	6758± 9	0.60± 0.01	2.95± 0.02	4.33± 0.02	4.41± 0.03
003727.78-731454.9	0.92± 0.01	1.53± 0.01	-0.88± 0.16	6755± 8	0.59± 0.01	2.95± 0.01	4.29± 0.02	4.38± 0.02
005728.85-723454.6	0.93± 0.02	1.52± 0.01	-0.76± 0.21	6739±10	0.57± 0.01	2.94± 0.02	4.26± 0.02	4.36± 0.03
005728.85-723454.6	0.93± 0.02	1.52± 0.01	-0.76± 0.21	6739±10	0.57± 0.01	2.94± 0.02	4.26± 0.02	4.36± 0.03
005026.32-732418.2	0.94± 0.02	1.52± 0.01	-1.00± 0.20	6653± 9	0.60± 0.01	2.94± 0.02	4.39± 0.02	4.48± 0.03
004639.18-731324.7	0.89± 0.02	1.54± 0.01	-0.81± 0.20	6800±10	0.56± 0.01	2.93± 0.02	4.29± 0.02	4.42± 0.03
003816.46-732449.2	0.92± 0.02	1.52± 0.01	-0.74± 0.19	6738± 9	0.55± 0.01	2.93± 0.02	4.29± 0.02	4.42± 0.03
005110.48-730750.0	0.87± 0.01	1.55± 0.01	-0.85± 0.18	6805± 9	0.55± 0.01	2.92± 0.02	4.33± 0.02	4.48± 0.03
010452.90-724025.9	0.95± 0.01	1.52± 0.01	-1.00± 0.19	6599± 9	0.59± 0.01	2.92± 0.02	4.44± 0.02	4.55± 0.03
005646.16-723452.2	0.88± 0.01	1.55± 0.01	-1.06± 0.18	6691± 9	0.57± 0.01	2.90± 0.02	4.48± 0.02	4.65± 0.03
005957.83-730647.6	0.87± 0.01	1.55± 0.01	-0.99± 0.17	6717± 8	0.56± 0.01	2.90± 0.01	4.44± 0.02	4.63± 0.03
005458.09-724948.9	0.89± 0.01	1.55± 0.00	-1.11± 0.15	6646± 7	0.58± 0.01	2.90± 0.01	4.51± 0.01	4.68± 0.02
004758.98-732241.3	0.89± 0.02	1.54± 0.01	-0.95± 0.26	6683±12	0.56± 0.01	2.90± 0.02	4.45± 0.03	4.63± 0.04
010535.93-720621.6	0.94± 0.02	1.53± 0.01	-0.98± 0.30	6583±13	0.57± 0.01	2.89± 0.03	4.49± 0.03	4.67± 0.05
010516.55-722526.5	0.90± 0.02	1.53± 0.01	-0.76± 0.20	6702± 9	0.53± 0.01	2.89± 0.02	4.38± 0.02	4.59± 0.03
004721.26-731135.5	0.89± 0.01	1.55± 0.01	-1.02± 0.17	6640± 8	0.56± 0.01	2.88± 0.02	4.52± 0.02	4.73± 0.03
005504.67-731106.4	0.91± 0.01	1.54± 0.01	-1.08± 0.19	6583± 9	0.57± 0.01	2.88± 0.02	4.56± 0.02	4.76± 0.03
004306.71-733527.9	0.92± 0.02	1.53± 0.01	-0.89± 0.20	6605±10	0.54± 0.01	2.88± 0.02	4.49± 0.02	4.70± 0.03

Complete table is available in the electronic form.

Table 6. Physical parameters extracted from Fourier coefficients for 17 RRc variables. Errors represent the uncertainties in the Fourier parameters.

OGLE ID (1)	M_V (K98) (2)	$\log(L/L_\odot)$ (SC93) (3)	[Fe/H] (4)	T_{eff} (5)	M/M_\odot (6)	$\log g$ (7)	R/R_\odot (FD) (8)	R/R_\odot (Mar) (9)
005451.72-723850.4	0.85± 0.03	1.66± 0.02	-1.10± 0.17	7457±17	0.59± 0.19	3.00± 0.33	4.07± 0.03	4.19± 0.02
005115.64-724739.2	0.78± 0.04	1.67± 0.02	-1.21± 0.16	7425±17	0.62± 0.19	3.00± 0.31	4.19± 0.04	4.25± 0.02
010245.99-721132.7	0.83± 0.04	1.83± 0.03	-2.02± 0.11	7165±18	1.13± 0.07	3.04± 0.06	5.35± 0.05	4.63± 0.02
004631.02-724658.8	0.78± 0.04	1.75± 0.03	-1.67± 0.17	7266±20	0.77± 0.18	2.97± 0.24	4.79± 0.05	4.65± 0.02
004902.13-724513.6	0.82± 0.03	1.76± 0.02	-1.73± 0.13	7247±15	0.80± 0.18	2.97± 0.23	4.87± 0.04	4.69± 0.02
010453.59-723756.0	0.78± 0.03	1.83± 0.01	-2.11± 0.08	7115±10	0.93± 0.17	2.94± 0.18	5.44± 0.04	5.09± 0.01
010029.57-725454.2	0.77± 0.04	1.81± 0.02	-2.03± 0.09	7136±10	0.85± 0.19	2.93± 0.22	5.32± 0.05	5.10± 0.01
010029.57-725454.2	0.77± 0.04	1.81± 0.02	-2.03± 0.09	7136±10	0.85± 0.19	2.93± 0.22	5.32± 0.05	5.10± 0.01
004327.25-724542.4	0.76± 0.03	1.75± 0.02	-1.62± 0.13	7238±13	0.64± 0.22	2.89± 0.34	4.80± 0.04	4.96± 0.02
010231.17-722134.0	0.69± 0.04	1.83± 0.03	-2.13± 0.15	7107±18	0.91± 0.18	2.93± 0.19	5.46± 0.06	5.16± 0.02
005556.74-732133.6	0.77± 0.05	1.77± 0.03	-1.80± 0.17	7193±18	0.70± 0.21	2.89± 0.31	5.00± 0.06	5.07± 0.03
003934.35-730433.9	0.76± 0.03	1.79± 0.02	-1.92± 0.13	7161±13	0.76± 0.21	2.90± 0.28	5.16± 0.04	5.13± 0.02
010647.29-723053.7	0.73± 0.04	1.81± 0.02	-2.03± 0.13	7124±14	0.77± 0.21	2.88± 0.27	5.31± 0.04	5.27± 0.02
005155.37-724909.5	0.73± 0.04	1.77± 0.02	-1.78± 0.17	7183±16	0.65± 0.23	2.86± 0.35	5.00± 0.05	5.19± 0.03
010316.37-724816.2	0.66± 0.12	1.90± 0.03	-2.56± 0.13	6968±18	1.14± 0.12	2.92± 0.11	6.20± 0.15	5.54± 0.02
010316.37-724816.2	0.66± 0.12	1.90± 0.03	-2.56± 0.13	6968±18	1.14± 0.12	2.92± 0.11	6.20± 0.15	5.54± 0.02
005527.97-724136.8	0.76± 0.04	1.81± 0.03	-2.03± 0.16	7118±17	0.75± 0.22	2.87± 0.29	5.32± 0.05	5.35± 0.03

Kovács, G., Kupi, G. 2007, A&A, 462, 1007

Lázaro, C., Arellano Ferro, A., Arévalo, M. J. et al. 2006, MNRAS, 372, 69

Marconi, M., Nordgren, T., Bono, G. et al. 2005, ApJ, 623, L133

Morgan, S. M., Simet, M., Bagenquast, 1998, Acta Astron., 48, 341 (MSB98)

Morgan, S. M., Wahl, J. N., Wieckhorst, R. M., 2006, MmSAI, 77, 178

Morgan, S. M., Wahl, J. N., Wieckhorst, R. M., 2007, MNRAS, 374, 1421

Nemec, J., M., 2004, AJ, 127, 2185

Peña, J. H., Arellano, A., Sareyan, J. P., Peña, R., Alvarez,

M. 2007, Comm. in Asteroseismology, 150, 385

Petersen, J. O., 1986, A&A, 170, 59

Press, W., Teukolsky, S., Vetterling, W., Flannery, B. 1992, Numerical Recipes in FORTRAN (2nd ed.; Cambridge: Cambridge Univ. Press)

Pritzl, B. J., Armandroff, T. E., Jacoby, G. H., Da Costa, G. S., 2005, AJ, 129, 2232

Saha, A., Hoessel, J. G., 1990, AJ, 99, 97

Sakai, S., Ferrarese, L., Kennicutt, R. C. et al., 1999, ApJ, 523, 540

Salaris, M., Chieffi, A., Straniero, O., 1993, ApJ, 350, 645

Sandage, A., 2004, AJ, 128, 858

Schaltenbrand, R., Tammann, G., 1971, A&AS, 4, 265

- Sekiguchi, M., Fukugita, M., 2000, AJ, 120, 1072
Simon, N. R., Clement, C. M., 1993, ApJ, 410, 526 (SC93)
Simon, N., Lee, A. 1981, ApJ, 248, 291
Smith, H. A., Silbermann, N. A., Baird, S., R., Graham, J. A., 1992, AJ, 104, 1430
Soszyński, I., Udalski, A., Szymański, M. et al., 2002, Acta Astron., 52, 369 (SZ02)
Walker A. R., 1994, AJ, 108, 555 (W94)
Walker A. R., Nemec, J. M., 1996, AJ, 112, 2026
Walker A. R., 1998, AJ, 116, 220
Walker, A. R., Mack, P., 1988, AJ, 96, 872
Zinn, R., West, M. J., 1984, ApJS, 55, 45